coatings

MDPI

Article

Effects of Rare Earth Elements on Properties of Ni-Base Superalloy Powders and Coatings

Chunlian Hu [1] and Shanglin Hou [2,*]

[1] Alloy Powder Co., Ltd., Lanzhou University of Technology, Lanzhou 730050, China; huchl2005@126.com
[2] School of Science, Lanzhou University of Technology, Lanzhou 730050, China
* Correspondence: houshanglin@163.com; Tel.: +86-138-9369-7556; Fax: +86-931-2757-394

Academic Editors: Niteen Jadhav and Andrew J. Vreugdenhil
Received: 25 October 2016; Accepted: 23 January 2017; Published: 16 February 2017

Abstract: NiCrMoY alloy powders were prepared using inert gas atomization by incorporation of rare earth elements, such as Mo, Nb, and Y into Ni60A powders, the coatings were sprayed by oxy-acetylene flame spray and then remelted with high-frequency induction. The morphologies, hollow particle ratio, particle-size distribution, apparent density, flowability, and the oxygen content of the NiCrMoY alloy powders were investigated, and the microstructure and hardness of the coatings were evaluated by optical microscopy (OM). Due to incorporation of the rare earth elements of Mo, Nb, or Y, the majority of the NiCrMoY alloy particles are near-spherical, the minority of which have small satellites, the surface of the particles is smoother and hollow particles are fewer, the particles exhibit larger apparent density and lower flowability than those of particles without incorporation, i.e., Ni60A powders, and particle-size distribution exhibits a single peak and fits normal distribution. The microstructure of the NiCrMoY alloy coatings exhibits finer structure and Rockwell hardness HRC of 60–63 in which the bulk- and needle-like hard phases are formed.

Keywords: rare earth; microstructure; alloy powder; coating

1. Introduction

Due to excellent weldability properties, surface stability, corrosion resistance, and mechanical properties at high temperature, nickel-based superalloys are widely used for gasturbine components and other applications, such as the base materials for hot components, e.g., hot parts of aerospace turbine engines [1]. Nickel-based coatings can function either as overlay coatings or asbond coats in a thermal barrier coating system. They are usually applied using thermal spraying processes, such as low-pressure plasma spraying (LPPS), high velocity oxygen fuel spraying (HVOF), vacuum plasmas praying (VPS) and atmospheric plasma spraying (APS) [2]. All types of spraying processes use powder as feedstock, which typically results in a characteristic splat-structure [3].

Incorporation of rare earth (RE) elements into alloys may improve their high-temperature oxidation resistance or other mechanical properties. Chromium and aluminum are added to promote resistance to oxidation and hot corrosion. Incorporation of minor amounts of rare earth elements, such as Ce, Y, Zr, La, or their oxides enhance the bonding strength of the oxide layer [4] and improve the high-temperature oxidation resistance of alumina- and chromia-forming alloys [5]. Stringer [6] suggested the enhancement of oxide nucleation processes through the presence of rare earth elements. Antill and Peakall [7] reported that the beneficial effect of the rare earth elements was primarily to improve scale plasticity for accommodating stresses due to the difference in the thermal expansion coefficients between the alloy and the oxide scale. Tien and Pettit [8] concluded that the application of rare earth elements provide sites for vacancy condensation in an Fe–25Cr–4Al alloy, with consequent improvement of scale adhesion. It was reported that the rare earth elements, such as La, Y, Ce, and their oxides, can be used for reducing the oxidation rate and improving corrosion resistance of the

superalloys [9]. It was also found that high-density, fine, and uniform structure is formed in coatings deposited by Ni-based alloy powders with the addition of rare earth elements so as to improve the wear and corrosion resistance of Ni-based alloys [10]. Recently He [11] reported the microstructure and hot corrosion resistance of Co–Si-modified aluminide coating on nickel-based superalloys, and interdiffusion between a polycrystalline nickel-based superalloy (René 80) and two MCrAlY bondcoats, each with a different chemical composition, is demonstrated in [12].

Ni-based self-fluxing alloy powder Ni60A is one of the most important protective coating materials owing to excellent high-temperature corrosion resistance, and the coating sprayed by Ni60A powders with the incorporation rare earth elements, such as W and Mo, has better wear resistance [13]. It is well known that the properties of the powders influence characteristics of sprayed coatings extensively [14–16]. For example, both oxygen content and flowability of powders may induce porosity, impurities, or cracks in the coatings [17].

In this work, NiCrMoY alloy powders were prepared by using inert gas atomization with incorporation of rare earth elements, such as Mo, Nb, and Y into Ni60A powders, the coatings were sprayed by oxy-acetylene flame spray and then remelted with high-frequency induction. The morphologies, hollow particle ratio, particle-size distribution, apparent density, flowability, and oxygen content of NiCrMoY alloy powders were investigated, and the microstructure and hardness of the NiCrMoY-sprayed coatings are presented. The research results show that the properties of NiCrMoY alloy powders are improved due to the incorporation of rare earth elements, and the microstructure of NiCrMoY alloy coatings exhibit fine structure and Rockwell hardness HRC of 60–63.

2. Experimental Procedure

2.1. Preparation and Property Test of Powders

The Ni60A and NiCrMoY alloy powders were prepared by double-stage coupling fast freezing and low-pressure gas atomizing with an atomizing gas pressure of 5–10 MPa, the melt overheating temperature is 100–150 °C, and the particles had a near spherical morphology with internal pores and a size of 40–110 μm. The chemical compositions of the Ni60A alloy and NiCrMoY alloy powders are shown in Table 1 which was measured at the Testing Center of the Shanghai Research Institute of Materials according to ASTM E1019-11 [18], ASTM E2594-09(2014) [19], ASTM E354-14 [20], and ISO4938:1988 [21].

Table 1. Chemical compositions of the NiCrMoY and Ni60A alloy powders (wt %).

Alloy	Chemical Compositions									
	C	**B**	**Si**	**Cr**	**Fe**	**Mo**	**Cu**	**Nb**	**Y**	**Ni**
Ni60A	0.98	2.91	3.96	16.4	3.2	–	–	–	–	Bal.
NiCrMoY	1.0	2.85	4.0	16.5	3.0	2.5	1.5	0.5	0.15	Bal.

The epoxy resin and the ethidenediamine were mixed proportionally with the Ni60A and NiCrMoY alloy powders, respectively, and then polished a cross-section to test the porosity of the powder after the epoxy resin solidified. The morphologies of powders were examined by a Reicher-Jung (Leica MeF3) optical microscope (OM) (Leica Microsystems, Wetzlar, Germany). A Mastersizer 2000 laser diffraction particle size analyzer (Malvern Instruments Ltd., Malvern, UK) was performed to analyze particle-size distribution. The apparent density and flowability of two kinds of powders were carried out with a FL4-1-type Hall flowmeter (Baishan Jiujiu Instruments Ltd., Baishan, Jilin, China). The oxygen content was measured with aTCH600 hydrogen-nitrogen-oxygen analyzer (LECO Corporation, St. Joseph, MI, USA).

2.2. Preparation and Property Test of Coatings

The Ni60A and NiCrMoY alloy powders were sprayed onto a degreased and grit-blasted mild 45# steel rod substrate of Φ 50 mm × 200 mm in size, to a thickness of 1.8 mm by oxy-acetylene flame spray and high-frequency induction remelting. The substrate was preheated and acetylene was used as the fuel gas. The spraying parameters are presented in Table 2. After being sprayed and cooled, the samples were cut with a size of 10 mm × 10 mm × 1.5 mm, and then polished using 400–1200# SiC waterproof abrasive paper, cleaned in alcohol, and corroded for 5–6 s in aqua regia.

Table 2. Oxy-acetylene flame spraying parameters.

Parameters	Gas	
	O_2	C_2H_2
Pressure (MPa)	1.2	0.1
Flow rate (m^3/h)	1.6–1.8	1.2–1.5
Spray rate (kg/h)	7.0	
Spray distance (mm)	150–200	
Thickness (mm)	250	
Remelting voltage (V)	550	
Remelting current (A)	280	

An optical microscope (OM) was used to characterize the microstructure of the Ni60A and NiCrMoY alloy sprayed coatings. The hardness of the sprayed coatings was evaluated with aHRMS-45 digital Rockwell hardness tester.

3. Results and Discussion

3.1. Properties of Powders

The morphologies of the NiCrMoY alloy powders and the Ni60A alloy powders are shown in Figure 1a,b, respectively. It can be seen that the NiCrMoY powders and Ni60A powders are near-spherical, but the sphericity of the NiCrMoY powders is better than that of the Ni60A powders, and a small number of the NiCrMoY powders have small satellites, while the Ni60A powders have more joint structures.

It is well know that morphology of powders depends on the surface tension of alloy melt, cooling speed, and shrinkage time. Better sphericity and the smoother surface of the powders are formed owing to the increasing surface tension, slow cooling speed, and long shrinkage time [22]. Due to incorporation of high melting point alloy elements, such as Mo and Nb, into the NiCrMoY powders, the melting point of NiCrMoY powders increases and particle surface tension becomes larger than the powders without addition, i.e., Ni60A alloy powders. Meanwhile the addition of Cu and rare earth Y makes the grains' surface smooth, improves the malleability [23], and there is enough time and energy to form a better spherical shape and smoother surface for the NiCrMoY alloy grains (as shown in Figure 1a) during the formation process of the powders by double-stage coupling fast freezing and low-pressure gas atomizing.

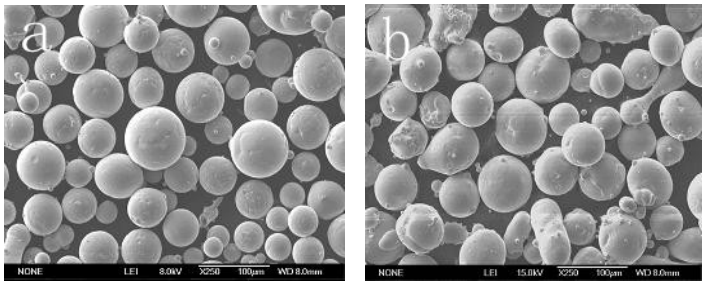

(**a**) (**b**)

Figure 1. Morphologies of (**a**) the NiCrMoY Powders and (**b**) the Ni60A Powders.

When the particles come out of the nozzle and are atomized by low-pressure gas atomization, the large particles get cooled slowly and have a higher temperature than the small ones, thus, small particles adhere to the surface of the large ones to form joint structure and satellite. Moreover the Ni60A powders easily adhere to the small particles because of its low melting point, so that Ni60A alloy powders have a poor rate of sphere formation and have satellites, as shown in Figure 1b.

The porosity of the powders can be expressed by the hollow particle ratio of the particles to the ones without porosity in terms of unit area of the cross-section of the powder sample. Figure 2a,b show the cross-section of NiCrMoY alloy powders and Ni60A alloy powders, respectively, but the samples in Figure 2 were gradually ground and polished without corrosion. It can be seen that the hollow particle ratio of NiCrMoY alloy powders is 6.5%, which is lower than 12.5% forNi60A alloy powders. This is because the rare earth elements interact with oxygen in the alloy melt to form tiny and dispersive rare earth compounds, and Y enhances the non-oxidizability and malleability of the alloy.

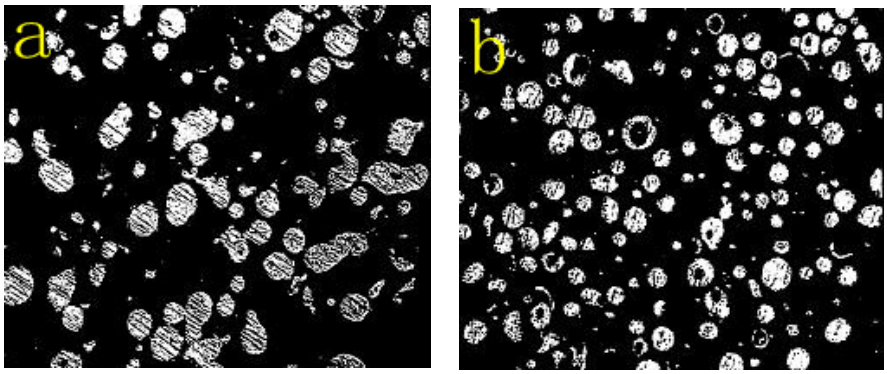

Figure 2. Cross-section of (**a**) NiCrMoY powders and (**b**) Ni60A powders.

Although deoxidization and degasification are carried out in the melting process, there is still small amounts of air existing in the alloy melt, and the temperature and pressure of the atomizing gas (nitrogen) in the atomization barrel increases rapidly during the atomization process, so the cooling velocity of alloy droplets slows so that more gas comes out from the alloy liquids. Meanwhile, due to the stirring induced by the high-pressure, some alloy powders contain nitrogen in the particle-forming process to form porosity in the particles [24]. However, the hollow particles are easy to burst and form pinholes in the coating layer when spraying. This is an important factor which influences the quality of the coatings, so the hollow particle ratio should be reduced as much as possible.

The particle-size distribution of the NiCrMoY and Ni60A alloy powders are carried out for an appropriate dispersing agent and the dispersion time is shown in Figure 3a,b, respectively. It can be seen from Figure 3a that the particle-size distribution of the NiCrMoY alloy powders shows a single peak and fits a normal distribution, and most of particle sizes are in the 38.59–118.15 μm range, and the median particle diameter d is 68.3 μm. Figure 3b shows the particle-size distribution of the Ni60A powders, which is bimodal, dispersive, and has a larger median particle diameter.

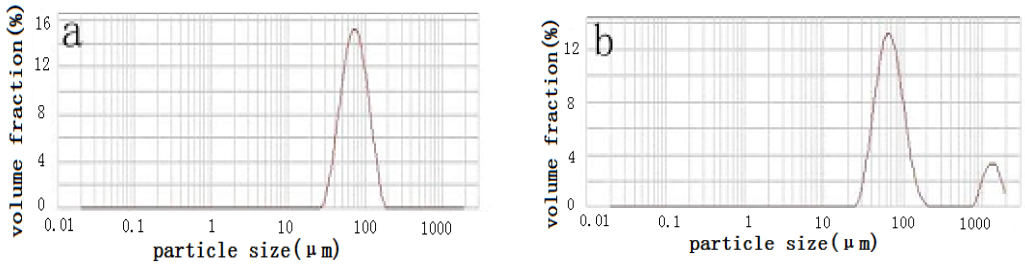

Figure 3. Particle size distribution of (**a**) NiCrMoY powders and (**b**) Ni60A powders.

The NiCrMoY alloy powder has a higher melting point and increasing surface tension due to the addition of the high melting-point alloy, such as Mo or Nb; thus, it requires more energy during gas atomization and the powder size increases compared to those without addition under the same atomizing parameters. However, because the Ni60A alloy powders have many joint structures and satellites, the particle size distribution of Ni60A powders is bimodal and dispersive, as shown in Figure 3b.

Figure 4 shows the apparent density and flowability of the NiCrMoY alloy powders and the Ni60A alloy powders. The apparent density and flowability of the NiCrMoY powders are 4.300 g/cm^3 and 14.07 s/50 g, respectively, while those of the Ni60A powders are 4.031 g/cm^3 and 15.05 s/50 g. Thus, it can be seen that the apparent density and flowability of the NiCrMoY alloy powders are better than those of Ni60A alloy powders.

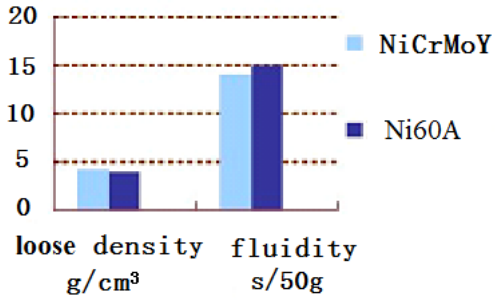

Figure 4. The apparent density and flowability of the powders.

The apparent density and flowability of powders depend on particle-size distribution, morphology, hollow particle ratio, and so on. The flowability of powders increases with better sphericity, and the apparent density of powders increases with the decreasing hollow particle ratio; high apparent density induces particle-size distribution dispersion in spite of large or small powders. This is in good agreement with the particle-size distribution, morphology, and the hollow particle ratio of the two kinds of powders mentioned above.

Figure 5 reveals the oxygen content of the NiCrMoY alloy powders and the Ni60A alloy powders, respectively. The oxygen content of the NiCrMoY alloy powders is 0.042%, lower than that of the 0.072% of the Ni60A powders. This is because rare earth Y improves the non-oxidizability of the alloy powders. The oxygen content of powders has a noticeable effect on the property of the sprayed coatings, and induces defects in coatings, so it should be reduced as much as possible.

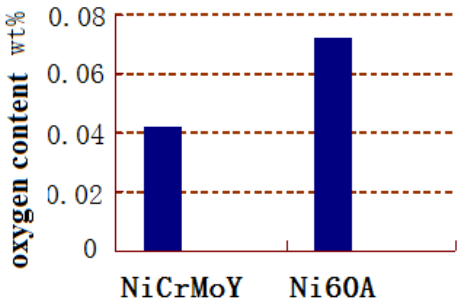

Figure 5. The oxygen content of the powders.

3.2. Properties of Coatings

The microstructure of coatings of the NiCrMoY alloy powders and the Ni60A alloy powders are shown in Figure 6a,b, respectively. As shown in Figure 6a, boride and carbide structures are distributed in the austenitic matrix of the Ni60A alloy coating. Not only boride and carbide structures be seen

from Figure 6b, but also many needle-like hard phases that are uniformly distributed in the austenitic matrix of the NiCrMoY alloy coating. This is because Mo is a kind of refractory metal with large atomic radius, which can induce noticeable distortion in the crystal lattice of the nickel solid solution. It is reported that carbide is formed uniformly due to the incorporation of the rare earth elements so as to improve the mechanical property of the alloy, especially its shock property [25,26].

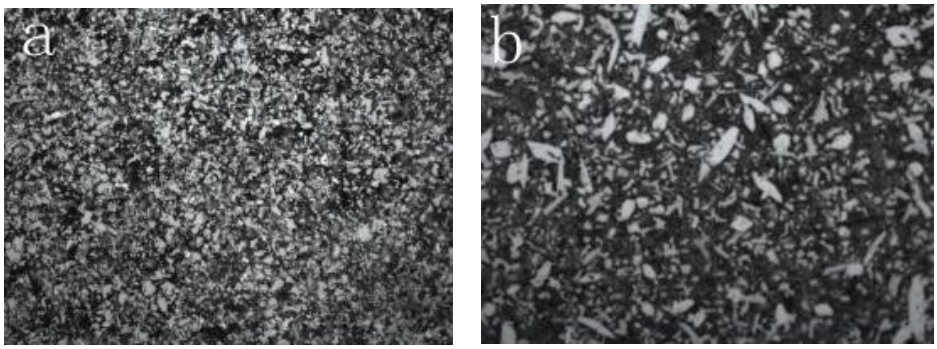

Figure 6. Microstructure of (**a**) the Ni60A coating and (**b**) the NiCrMoY coating.

The test results of hardness of the Ni60A coating and the NiCrMoY alloy coating are shown in Table 3. It can be seen that the hardness of the NiCrMoY alloy coating is higher. This is because the addition of the Mo element of the NiCrMoY coating causes grain refinement, increased toughness, decreased crack sensitivity, and enhanced high-temperature hardness and wear resistance. The addition of Nb strongly forms carbide and effectively refines grains. Thus, the appropriate incorporation of rare earth elements refines alloy structures, eliminates impurities, and forms the hard phases, such as carbide and boride, to prevent other new hard phases from forming. This causes the block- and needle-like hard phases to be uniformly distributed in alloy coatings, which increases the hardness of the alloy coatings

Table 3. Hardness of the Ni60A coating and NiCrMoY coating.

Coatings	HRC					
	1	**2**	**3**	**4**	**5**	**Average**
Ni60A	60.5	60.5	61.0	60.0	60.5	60.5
NiCrMoY	62.0	62.5	63.0	62.5	63.0	62.6

4. Conclusions

- Due to the incorporation of the rare earth elements Mo, Nb, or Y, the majority of the NiCrMoY alloy particles exhibit better sphericity, smoother surface, fewer joint structures, larger apparent density, and lower flowability than those of particles without incorporation.
- The particle-size distribution of NiCrMoY alloy powders shows a single peak and fits a normal distribution with a median particle diameter of 68.3 μm, an apparent density of 4.300 g/cm^3, and a flowability of 14.07 s.
- The microstructure of the NiCrMoY alloy coatings exhibits a finer structure and better hardness by the incorporation of appropriate amounts of Mo and Nb, and small amount of Y elements.

Acknowledgments: This work was financially supported by the National Natural Science Foundation of China (Grant Nos. 61665005 and 61367007) and the Natural Science Foundation of Gansu province of China (Grant No. 1112RJZA018).

Author Contributions: Chunlian Hu conceived, designed and performed the experiments; Shanglin Hou analyzed the data and wrote the paper.

Conflicts of Interest: The authors declare no conflict of interest.

References

1. Tsai, Y.L.; Wang, S.F.; Bor, H.Y.; Hsu, Y.F. Effects of Zr addition on the microstructureand mechanical behavior of a fine-grained nickel-based superalloy at elevated temperatures. *Mater. Sci. Eng. A* **2014**, *607*, 294–301. [CrossRef]
2. Scrivani, A.; Bardi, U.; Carrafiello, L.; Lavacchi, A.; Niccolai, F.; Rizzi, G. A comparative study of high velocity oxygen fuel, vacuum plasma spray, and axial plasma spray for the deposition of CoNiCrAlY bond coat alloy. *J. Therm. Spray Technol.* **2003**, *12*, 504–507. [CrossRef]
3. Safai, S.; Herman, H. Microstructural investigation of plasma-sprayed aluminum coatings. *Thin Solid Films* **1977**, *45*, 295–307. [CrossRef]
4. Christensen, R.J.; Tolpygo, V.K.; Clarke, D.R. The influence of the reactive element yttriumon the stress in alumina scales formed by oxidation. *Acta Mater.* **1997**, *45*, 1761–1766. [CrossRef]
5. Paul, A.; Elmrabet, S.; Odriozola, J.A. Low cost rare earth elements deposition method for enhancing the oxidation resistance at high temperature of Cr_2O_3 and Al_2O_3 forming alloys. *J. Alloys Compd.* **2001**, *323*, 70–73. [CrossRef]
6. Stringer, J.; Wallwork, G.R.; Wilcox, B.A.; Hed, A.Z. Effect of a thoria dispersion on high-temperature oxidation of chromium. *Corros. Sci.* **1972**, *12*, 625–636. [CrossRef]
7. Antill, J.; Peakall, K. Influence of an alloy addition of yttrium on the oxidation behavior of an austenitic and a ferritic SS in carbon dioxide. *J. Iron Steel Inst.* **1967**, *205*, 1136–1142.
8. Tien, J.K.; Pettit, F.S. Mechanism of oxide adherence on Fe–25Cr–4Al(Y or Sc) alloys. *Metall. Trans.* **1972**, *3*, 1587–1599. [CrossRef]
9. Thanneeru, R.; Patil, S.; Deshpande, S. Effect of trivalent rare earth dopants in nanocrystalline ceria coatings for high-temperature oxidation resistance. *Acta Mater.* **2007**, *55*, 3457–3466. [CrossRef]
10. Xiu, S.; Lei, W.; Yang, L. Effects of temperature and rare earth content on oxidation resistance of Ni-based superalloy. *Prog. Nat. Sci. Mater. Int.* **2011**, *21*, 227–235.
11. He, H.; Liu, Z.; Wang, W.; Zhou, C. Microstructure and hot corrosion behavior of Co–Si modified aluminide coating on nickel based superalloys. *Corros. Sci.* **2015**, *100*, 466–473. [CrossRef]
12. Elsaß, M.; Frommherz, M.; Scholz, A.; Oechsner, M. Interdiffusion in MCrAlY coated nickel-base superalloys. *Surf. Coat. Technol.* **2016**, *307*, 565–573. [CrossRef]
13. Tan, J.; Looney, L.; Hashmi, M. Component repair using HVOF thermal spraying. *J. Mater. Process. Technol.* **1999**, *92*, 203–208. [CrossRef]
14. Hu, C.; Hou, S. Failure analysis of plungers sprayed by Ni-based alloy on hydraulic feedback subsurface pump. *J. Chin. Soc. Corros. Prot.* **2012**, *32*, 80–84.
15. Dong, G.; Yan, B.; Deng, Q.; Yu, T. Effect of niobium on the microstructure and wear resistance of nickel-based alloy coating by laser cladding. *Rare Metal Mater. Eng.* **2011**, *40*, 973–977.
16. Tang, Y.; Yang, J. Influence of rare earth on wear ability of spray welding layer. *Hot Work. Technol.* **2001**, *1*, 32–33.
17. Lu, Z.; Tian, Y.; Zhu, C. Study on Ni60AA alloy powder coating by high frequency induction heating thermal. *Spray Technol.* **2012**, *4*, 44–46.
18. *ASTM E1019-11 Standard Test Methods for Determination of Carbon, Sulfur, Nitrogen, and Oxygen in Steel, Iron, Nickel, and Cobalt Alloys by Various Combustion and Fusion Techniques*; ASTM International: West Conshohocken, PA, USA, 2011.
19. *ASTM E2594-09 Standard Test Method for Analysis of Nickel Alloys by Inductively Coupled Plasma Atomic Emission Spectrometry (Performance-Based Method)*; ASTM International: West Conshohocken, PA, USA, 2014.
20. *ASTM E354-14 Standard Test Methods for Chemical Analysis of High-Temperature, Electrical, Magnetic, and Other Similar Iron, Nickel, and Cobalt Alloys*; ASTM International: West Conshohocken, PA, USA, 2014.
21. *ISO 4938 Steel and Iron-Determination of Nickel Content-Gravimetric or Titrimetric Method*; International Organization for Standardization: Geneva, Switzerland, 1988.
22. Wang, Y.; Shen, D.; Liao, B. Effect of rare earth on Ni-based spontaneous melting alloy by laser cladding. *Appl. Laser* **2003**, *3*, 139–141.
23. Zhang, C. Research on RE Micro-Alloy Effect in Self-Fusion Alloy. Master's Thesis, Shenyang University of Technology, Shenyang, Liaoning, China, 2005.

24. Liang, B.; Zhang, Z. Development and application in Ni-based powders containing rare earth elements. *J. Lanzhou Polytech. Coll.* **2007**, *1*, 28–30.
25. Ma, Y.; Huang, B.; Fan, J. Effect of rare earth Y on preparation of nanometer W-Ni-Fe composite powder. *Rare Metal Mater. Eng.* **2005**, *34*, 1135–1138.
26. Yuan, H.; Li, Z.; Xu, W. The study of Argon atomized superalloy powders. *Powder Metall. Ind.* **2010**, *4*, 1–5.